Some characteristics of the concert harp's acoustic radiation

Jean-Loic Le Carrou[a)]
LAM/IJLRA, UMR CNRS 7190, UPMC Univ. Paris 06, 11 rue de Lourmel 75015 Paris, France

Quentin Leclere
Laboratoire Vibrations Acoustique—INSA Lyon, 25 bis Avenue Jean Capelle 69621 Villeurbanne Cedex, France

Francois Gautier
LAUM, UMR CNRS 6613, Université du Maine, Avenue Olivier Messiaen 72085 Le Mans, France

(Received 17 July 2009; revised 22 December 2009; accepted 9 March 2010)

The way a musical instrument radiates plays an important part in determining the instrument's sound quality. For the concert harp, the soundboard has to radiate the string's vibration over a range of 7 octaves. Despite the effort of instrument makers, this radiation is not uniform throughout this range. In a recent paper, Waltham and Kotlicki [J. Acoust. Soc. Am. **124**, 1774–1780 (2008)] proposed an interesting approach for the study of the string-to-string variance based on the relationship between the string attachment position and the operating deflection shapes of the soundboard. Although the soundboard vibrational characteristics determine a large part of the instrument's radiation, it is also important to study directly its radiation to conclude on the origins of the string-to-string variation in the sound production. This is done by computing the equivalent acoustical sources on the soundboard from the far field sound radiation measured around the harp, using the acoustic imaging technique inverse frequency response function. Results show that the radiated sound depends on the correlation between these sources, and the played string's frequency and location. These equivalent sources thus determine the magnitude and directivity of each string's partial in the far field, which have consequences on the spectral balance of the perceived sound for each string. © *2010 Acoustical Society of America.* [DOI: 10.1121/1.3377055]

PACS number(s): 43.75.Gh [NHF] Pages: 3203–3211

I. INTRODUCTION

The harp is a string instrument with many variations, whose geometry and string tuning mechanism can be different according to the type: small Welsh, Irish, Scottish, Celtic, and Concert harps. The latter, with a larger size than the others, is currently used in symphonic orchestras and is the subject of the present study. From an acoustical point of view, the concert harp is a complex sound source involving coupling between a set of strings, a flat panel called the soundboard, and a cavity with five sound holes called the sound box. The musical sound field produced by the instrument has a complex spatial distribution linked to its sound directivity. The aim of the present paper is to study the acoustic radiation in order to give some characteristics of the sound directivity when the harp is played.

In a recent paper,[1] Waltham and Kotlicki proposed an interesting study of the vibrational characteristics of harp soundboards. Their work deals with the relationship between characteristics of the strings (the fundamental frequencies and the attachment positions) and characteristics of the mechanical admittance of the soundboard (which depend on frequency and on location, and whose maximum and minimum indicate anti-nodes and nodes, respectively). Since the coupling between the strings and the soundboard is governed by the mechanical admittance, the authors have shown that "coincidences between string fundamental frequencies and the anti-nodes of the soundboard correlate with excessively loud strings; coincidences between string fundamental frequencies and the nodes of the soundboard correlate with 'dead' strings." This characteristic is important for the instruments' maker who wants to design an instrument, which do not have an excessive string-to-string variation in sound radiation while having a reasonably high overall sound radiation level. Their results show that the variance in admittance at the string's connections from string to string is different for two kinds of harps. For a harp with a good radiativity and without a large string-to-string variance, they conclude that the string positions as a function of their fundamental frequencies are located just above the anti-node of the lowest mode and below the primary anti-nodes of the higher modes, when plotted in a map representing the admittance magnitude.

Although the vibrational characteristics of the soundboard determine a large part of the instrument's radiation, it is important to study, in addition, its radiation itself to determine the influence of the string-to-string variation in the sound production. This is the aim of this paper.

Few studies exist on the harp's radiation.[2] The first ones were concerned about the optimum position of microphones for sound recording and of the concert harp inside an orchestra.[3,4] To do that, the directivity of the instrument was measured by a single microphone moved around the instru-

[a)]Author to whom correspondence should be addressed. Electronic mail: jean-loic.le_carrou@upmc.fr

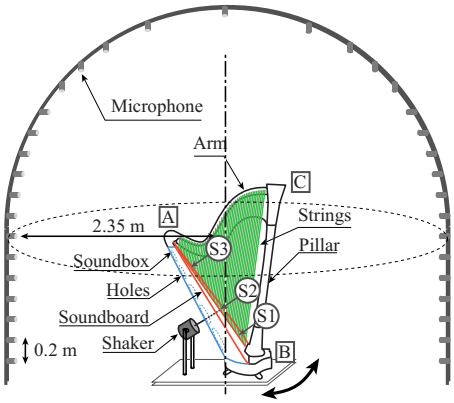

FIG. 1. (Color online) Experimental setup.

ment excited by a stationary source. Preferential directions for the far field sound radiation of the instrument over a wide range of frequencies are determined: three kinds of radiated sound fields, depending on the frequency, are found. In the low-frequency range (0–400 Hz), the harp is non-directional, in the medium frequency range (400–2000 Hz), the harp is directional with a high sound level on both the front and back sides of the instrument, and in the high frequency range (2000–4000 Hz), the instrument radiates more from the back and two major radiation areas are found on the front side. More recently, the vibroacoustic behavior of the concert harp was investigated in the low-frequency range.[5] The study shows the importance of two coupled modes both involving air motions inside the holes and the bending motion of the soundboard in the acoustic radiation of the instrument. A radiation model based on simple sources located on the soundboard and on the sound holes shows that this particular behavior can also be identified.[6] However, these two studies are limited in the low-frequency range (below 200 Hz), and the aim was not to investigate the sound radiation of the harp in a large frequency range in linking with the string-to-string acoustic variance.

In the present paper, we focus on the harp's far field radiation when it is played in connection with the soundboard's acoustical radiation. To do that, we first measure in a forced regime the sound field radiated by the harp 's acoustic radiation profile. Equivalent acoustical sources on the soundboard are then found by using an appropriate inverse frequency response function (IFRF) method. Finally, the link between these sources and string's location is studied in order to extend the results from Ref. 1.

II. FAR FIELD SOUND RADIATION

A. Experimental setup

The experimental setup shown in Fig. 1 is used to measure the far field directivity of a concert harp (*Camac Harps, Atlantide Prestige model*, France). Measurements are performed in a semi-anechoic room of working volume 1000 m^3, of valid frequency range of 70 Hz–20 kHz. The instrument is excited by a shaker driven by a white noise source, connected via a rod to the back of the soundboard. An arch contained in a vertical plane, on which 35 1/4-inch microphones are attached, is kept fixed, whereas the harp and its excitation apparatus rotate by 18 10° steps about the z-axis (see Fig. 1). With this setup, the radiated pressure of the harp in the half-space can be measured. Note that a 180° rotation is enough to obtain the sound field in the whole hemisphere.

The arch dimensions are 4.70 m in width and 3.55 m in height, enabling the positioning of microphones at a distance of 2.35 m from the rotating axis. Taking into account the size of the instrument, the distance between the microphones and the sound box of the harp is at least $r=2$ m. Since the far field approximation is valid for $k_0 r \gg 1$, with k_0 as the acoustic wavenumber, we can consider that it is satisfied for frequencies above 100 Hz. Moreover, the distance between two microphones was chosen to be 0.2 m in order to have a good measurement mesh resolution. According to Shannon's principle, this distance must not exceed a half wavelength on the measurement mesh. The difficulty is to correctly estimate the spatial frequency content of the acoustic field projected on the measurement mesh. In our case, the measurement grid is far enough from the source to assume the absence of evanescent components. Therefore we can consider that the maximum wavenumber of the two–dimensional information projected on the grid does not exceed the acoustic wavenumber. This would fix the upper limit of this study at 850 Hz. Moreover, this limit stands for plane waves traveling tangentially to the measurement mesh. If we consider that waves coming from the source cannot reach the measurement mesh with an angle of incidence θ greater than $\pi/2$, the upper frequency limit can be divided by $\sin(\theta)$. Considering $\theta=\pi/3$ (which is reasonable considering the geometry given in Fig. 1), the upper frequency limit can be widened to 1 kHz.

In order to study the dependency of the harp's radiation on the strings' locations, three positions on the soundboard of the shaker are used, denoted S1, S2, and S3 on Fig. 1:

- S1 location, between strings 41 ($G\flat_6$) and 42 ($F\flat_6$), fundamental frequencies at 46.2 and 41.2 Hz, respectively;
- S2 location, between strings 30 ($D\flat_5$) and 31 ($C\flat_5$), fundamental frequencies at 138.6 and 123.5 Hz, respectively;
- S3 location, between strings 11 ($B\flat_2$) and 12 ($A\flat_2$), fundamental frequencies at 932.3 and 830.6 Hz, respectively.

The force applied by the shaker (F) to the harp is measured using an appropriate force transducer. Therefore, for each pressure measurement at point i (P_i), the frequency response function P_i/F is obtained. This experimental setup with 613 measurement points is a compromise between practical limitations and a good spatial resolution for the sound field.

B. Results

In this section, the sound radiated by the harp is described. In Fig. 2, a typical frequency response function obtained at the microphone placed in front of the harp at 1.4 m in height is shown. Representative examples of the sound directivity of the instrument are shown in Fig. 3 for several selected frequencies (also indicated in Fig. 2). These directivity patterns are presented using two cross sections: a ver-

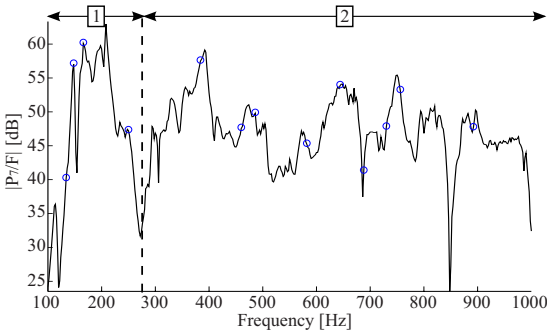

FIG. 2. (Color online) Frequency response function at the microphone placed in the plane containing the harp in the direction normal to the soundboard, on the measurement surface shown in Fig. 1, at a height of 1.4 m. Circles indicate frequencies of selected directivity patterns plotted in Fig. 3. The FRF is shown for the shaker located on S2 (Ref 1 dB: 2×10^{-5} Pa/N).

tical one on the strings plane and a horizontal one placed 1.4 m high. The triangle (ABC), as defined in Fig. 1, represents the orientation of the concert harp.

The 13 directivity patterns shown in Fig. 3 are symmetric with respect to the strings plane. The radiated sound is thus the same on each side of the instrument. This result is, of course, due to the fact that the instrument is excited on its central line along the soundboard and, so, no asymmetric modes of the soundboard could be excited. This result is expected in a playing configuration because strings are connected to the soundboard on this central line. These directivity patterns include the reflection of the radiated sound on the semi-anechoic room's floor. This reflection phenomenon can explain lobes or widenings in the low part of these patterns.

The description of the directivity patterns allows us to define two frequency ranges (labeled as 1 and 2 in Fig. 2). In range 1, below 220 Hz, the concert harp is non-directional, as shown in Fig. 3 for 134, 148, and 166 Hz (which, as presented in a previous study,[5] correspond respectively to T1 and A0 modes). In range 2, above 220 Hz, more complex patterns with lobes appear, as is the case from 250 to 892 Hz. In the horizontal cross section, lobes appear on the front and on the back of the instrument. Thus, a directivity dependency is not only found along the elevation angle but also along the azimuth angle. This result agrees with a straightforward experiment performed during the test: when a listener moves around the harp excited in forced regime at this frequency range, the instrument is nearly silent in some locations of the semi-anechoic room. In order to estimate the frequency at which the concert harp might be expected to pass from non-directional to directional, a common approximation is to consider the soundboard as a baffled piston, of radius a, for which the diffraction frequency[7] is $f=c/2\pi a$. The radius of the piston is approximated to the moving part of the soundboard in the low-frequency range. Then, the diffraction frequency for the concert harp with a radius of 20 cm is evaluated at approximately 270 Hz. This value is very close to the experimental value.

The results obtained here can be compared with those obtained from the qualitative study of the *Salvi Orchestra* concert harp by Bell and co-worker.[3,4] In this work, the directivity of the concert harp is studied using a third-octave analysis shown by a "3 dB plot" as introduced by Meyer.[8] First, the frequency limit at which their harp becomes non-

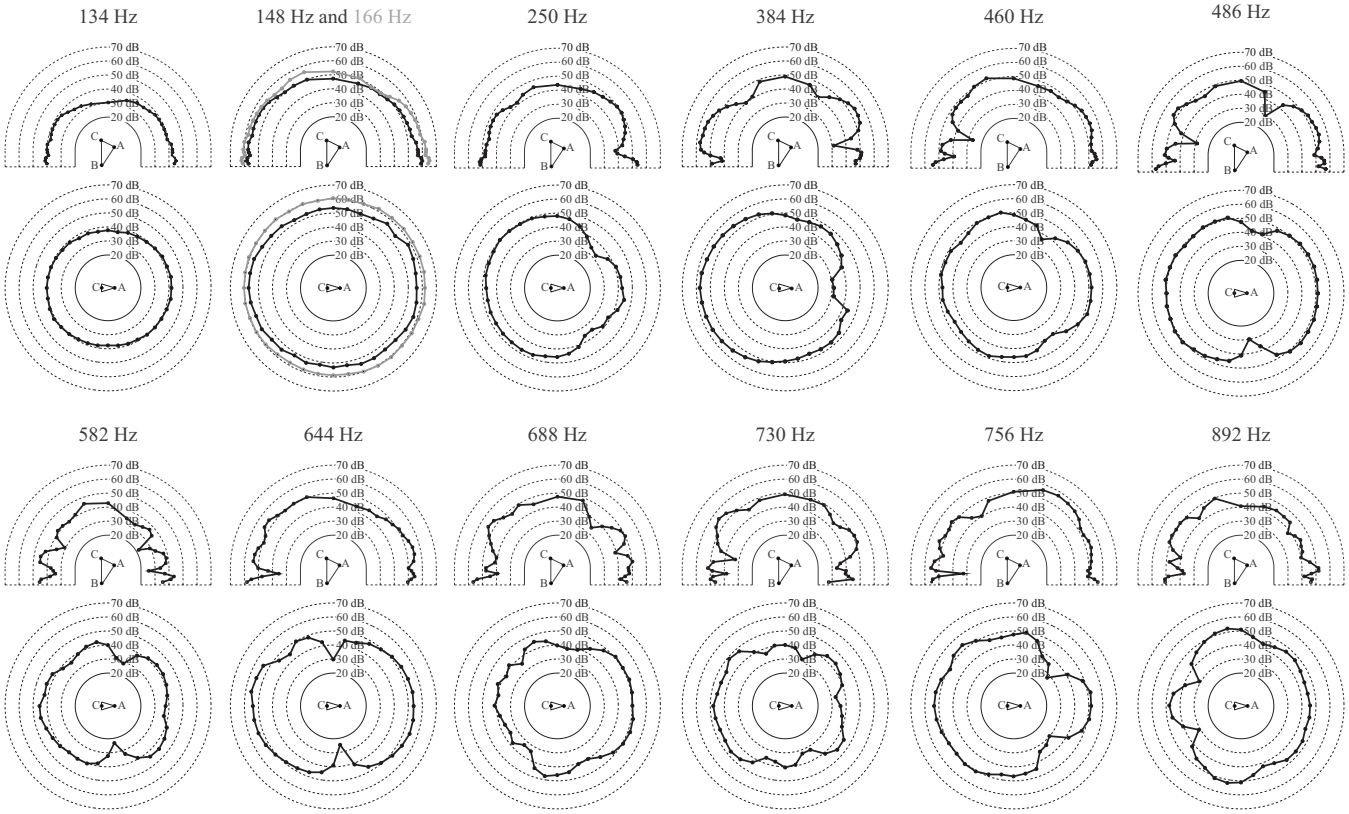

FIG. 3. Directivity pattern for 13 selected frequencies 134, 148, 166 (in gray), 250, 384, 460, 486, 582, 644, 688, 730, 756, and 892 Hz. Directivity patterns are shown for the shaker located on S2 (Ref 1 dB: 2×10^{-5} Pa/N).

directional is valued at 400 Hz, whereas for our concert harp with similar dimensions, this frequency is approximately 220 Hz. Moreover, the principal areas of radiation for different frequencies are found to be more complex in our study than those described by Bell and co-worker[3,4] (in the frequency range of 400–2000 Hz, the harp is directional with a high sound level on both the front and back sides of the instrument). In details, for some frequencies in the frequency range of 200–1000 Hz, the sound radiation principally comes from the front (250 and 384 Hz), the front and the back (460, 486, 582, 644, and 756 Hz), the back (688 Hz), and the front, the back and the sides (730 and 892 Hz), as shown in Fig. 3. Our results show that the angular radiation patterns seem to vary rapidly not only with direction but also with frequency. This characteristic, named "directional tone color" for the violin by Weinreich,[9] can produce some perceptible effects for the listener.

III. ACOUSTIC IMAGING METHOD

A. Introduction

The aim of acoustic imaging techniques is to localize and quantify acoustic sources using a microphone array. These techniques have been in constant progress during the last 30 years, since pioneer works from Billingley and Kinns[10] (for the beamforming) and Williams *et al.*[11] (for nearfield acoustical holography). These two approaches have been developed separately for different applications, the first one being based on far field measurements with a limited resolution in low frequency, and the second one based on nearfield measurements to take advantage of the evanescent waves enhancing the low-frequency resolution. A third approach that can be used for acoustic imaging consists in trying to reconstruct the measured acoustic radiation using equivalent sources.[12] The real source is represented by a set of simple acoustic sources (monopoles in most cases), and their volumetric velocities are identified using inverse methods.[13–15] This latter approach is used in this work to identify an equivalent source behaving like the concert harp.

B. Inverse FRF method

The relation between a given monopole and a microphone position in a semi-anechoic environment is expressed at the frequency ω by the following transfer function:

$$p(\omega) = \frac{j\rho\omega}{4\pi}\left(\frac{e^{-j\omega r/c}}{r} + \frac{e^{-j\omega r'/c}}{r'}\right)q(\omega) = (h(r) + h(r'))q(\omega) = Hq(\omega), \quad (1)$$

where r and r' stand for the distances from the microphone to the source and to its image resulting from reflections on the floor, respectively. The relation (1) can be expressed between a set of sources and a set of microphone positions, leading to a matrix expression of the acoustic radiation $\mathbf{p} = \mathbf{Hq}$. The inversion of this relation is highly ill-posed in low frequency, and a regularization procedure has to be implemented. A Tikhonov regularization is used in this work, and the regularization parameter is adjusted using an L-curve analysis.[16] The regularized solution is expressed by

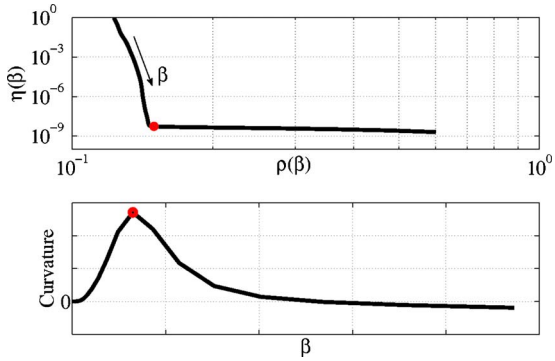

FIG. 4. (Color online) Top: L-curve at 200 Hz. bottom: curvature in function of β.

$$\mathbf{q}_\beta = (\mathbf{H}^*\mathbf{H} + \beta^2\mathbf{I})^{-1}\mathbf{H}^*\mathbf{p} \quad (2)$$

or

$$\mathbf{q}_\beta = \mathbf{V}(\mathbf{S} + \beta^2\mathbf{S}^{-1})^{-1}\mathbf{U}^*\mathbf{p}, \quad (3)$$

using the singular value decomposition (SVD) of the matrix $\mathbf{H}=\mathbf{USV}^*$, with $\mathbf{U}$ and $\mathbf{V}$ as orthogonal basis and $\mathbf{S}$ as a diagonal matrix. The SVD is used here because the L-curve analysis requires the computation of the solution for several values of β at each frequency. The use of Eq. (2) would require a matrix inversion for each β value. Using Eq. (3), the SVD is realized once for each frequency step.

The value of the regularization parameter β is chosen using the L-curve analysis,[16] an approach allowing to find the solution offering the best compromise between the minimization of the identified source strength and the minimization of the error on the reconstructed acoustic field. The L-curve represents the norm of the source strength in function of the norm of the error by varying β. The curvature of the L-curve is computed as follows:

$$c(\beta) = \frac{\eta''\rho' - \eta'\rho''}{(\eta'^2 + \rho'^2)^{3/2}},$$

$$\text{with} \quad \rho(\beta) = \log(\|\mathbf{p} - \mathbf{Hq}_\beta\|/\|\mathbf{p}\|),$$

$$\eta(\beta) = \log(\|\mathbf{q}_\beta\|/\|\mathbf{q}_0\|), \quad (4)$$

and where first and second derivatives of η and ρ are done with respect to β. The curvature is computed using finite difference schemes, based on the computation of η and ρ at a finite number of points of the L-curve. An example of L-curve and its curvature is given in Fig. 4 at 200 Hz. The circle stands for the corner of the curve found by maximizing its curvature: it corresponds to the optimal value of β.

Once volumetric velocities are estimated, their acoustic power has to be computed. The volumetric velocity of an equivalent source is indeed not directly comparable to the real source one: the identified volumetric velocities depends on the geometry and resolution of the source distribution. On the contrary, the resulting acoustic power on the source distribution is representative for the power of the real source.[17] The acoustic power of the monopole noted i can be computed as follows:

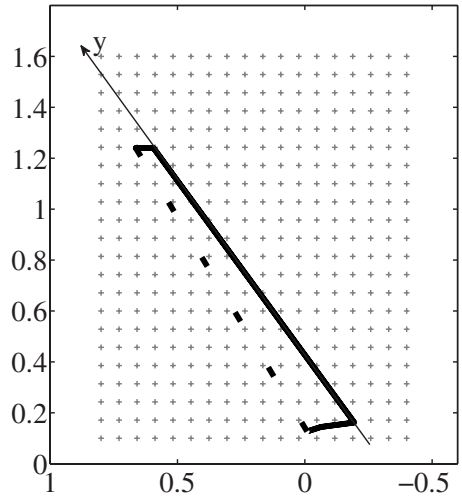

FIG. 5. Positions of elementary sources (grey+markers) in the harp's symmetry plane. The sound box profile is drawn in black.

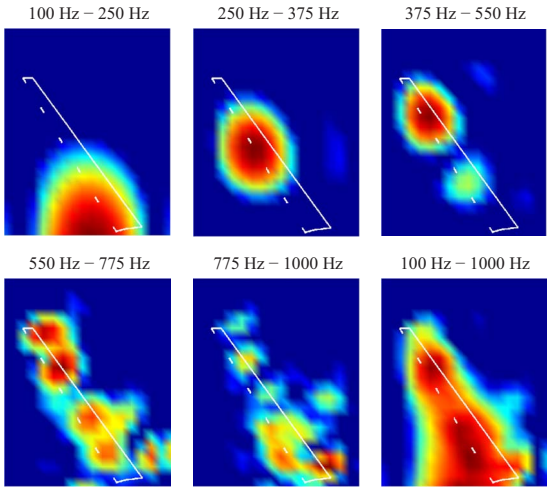

FIG. 6. (Color online) Acoustic power maps by frequency bands using IFRF. Images are drawn in dB using a 10 dB dynamic.

$$W_i = \frac{\rho\omega^2}{8\pi c}|q_i|^2 + \frac{\Re\{\tilde{p}_i\overline{q_i}\}}{2},$$

$$\text{with } \tilde{p}_i = h(R'_{ii})q_i + \sum_{k\in 1\ldots N, k\neq i}[h(R_{ik}) + h(R'_{ik})]q_k, \qquad (5)$$

where R_{ik} and R'_{ik} denoting the distances between monopoles i and k, and between the monopole i and the image of monopole k, respectively, and N is the total number of monopoles. $\tilde{p}_i$ is, in fact, the acoustic pressure generated by all monopoles except monopole i (but including its image on the floor) at its position.

C. Choice of the monopole's location

A key point of equivalent source methods consists in the restriction of source locations to those that are physically possible. In this study, we are interested in identifying acoustic sources on the harp from measurements in the far field. It is not possible in the frequency range of interest (100–1000 Hz) to separate different sources in the transversal dimension of the instrument. Moreover, the source exciting the soundboard is fixed on the central line, avoiding the radiation of asymmetric modes. The identification process is thus chosen to avoid identifications on the transversal axis, distributing monopoles on a rectangular surface in the symmetry plane of the harp. The dimensions of this source surface is 1.2 m horizontally and 1.5 m vertically, 396 monopoles are distributed with a resolution of about 7 cm ($\lambda/5$ at 1 kHz). The monopole positions are given in Fig. 5 together with the shape of the harp's sound box.

D. Results

Acoustic power maps are drawn in Fig. 6, integrated by frequency bands for excitation in S2. It can be seen on the last map [integrated on the whole frequency range of interest (100–1000 Hz)] that the acoustic power of the equivalent source clearly matches the location of the sound box.

Below 250 Hz, the acoustic power is located at the bottom of the sound box, centered on the floor. In this frequency band, the method is not able to separate the harp and its image on the floor. Between 250 and 375 Hz, the equivalent source is centered on the third hole, on the back side of the instrument. At 375 Hz, the equivalent source principally changes its position to the vicinity of the fourth hole, but a dipole behavior is also established with an out-of-phase contribution at the second hole height. Moreover, the sources are located at equivalent distances from the back and front sides of the sound box. From 375 Hz, only one acoustical equivalent source is not able to properly model the radiated sound of the concert harp, as already found in a previous study.[6] Nevertheless, from 100 to 550 Hz, the acoustical equivalent sources of the harp go up from the bottom to the top of the sound box. Between 550 and 750 Hz, the power is mostly located at the top of the sound board, as previously found by acoustic intensity measurements.[18] Above 750 Hz, the acoustic power seems to get back to the bottom of the harp, around the location of the shaker. Meanwhile, the resolution on the microphone grid is too poor for this frequency range, inducing potential erroneous ghost images on the map.[19]

IV. DISCUSSION AND INTERPRETATION

A. Acoustic power on the soundboard's central line

The main results of the imaging process concern the evolution in the frequency dependence of the identified acoustic power along the sound box's main axis. Thus, it would be helpful for the analysis to have a representation of this information in only one figure, giving the acoustic power density on the harp's axis in the frequency dependence. The acoustic power maps illustrated in Fig. 6 are thus integrated on the normal axis to the sound box's main axis (noted y in Fig. 5). For each position along the main axis y the acoustic power is computed using the following formula:

$$W^l(y) = \frac{1}{\Delta}\sum_{i\in\Omega(y)}\left[1 - \frac{|y_i - y|}{\Delta}\right]W_i, \qquad (6)$$

$\Omega(y)$ standing for the ensemble of elementary sources obeying the condition of $|y_i - y| < \Delta$, and Δ is a local half integration length along the y-axis. The resulting unit for W^l is

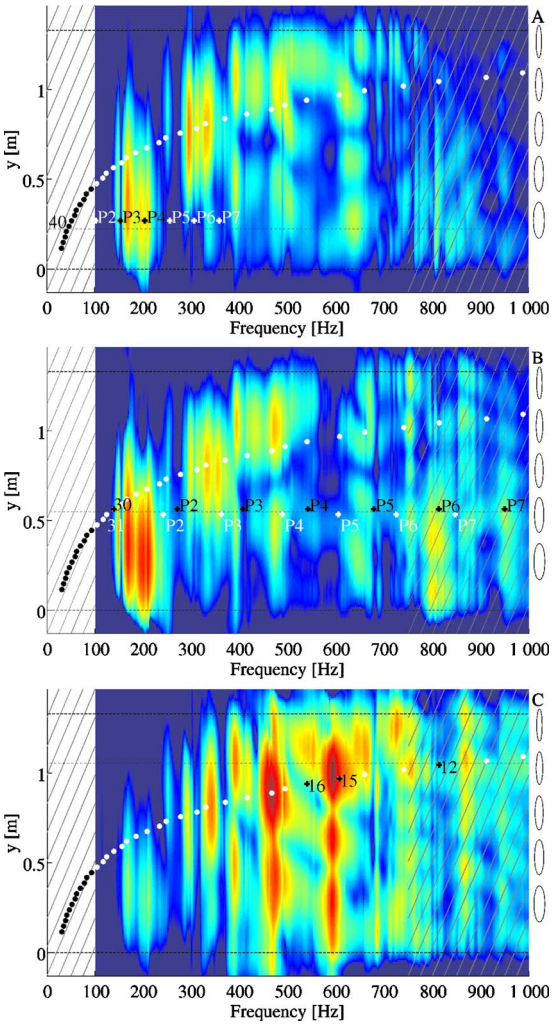

FIG. 7. (Color online) Acoustic power on the harp's central (y-axis) as a function of frequency (x-axis). Acoustic power maps are computed by using the IFRF method when the harp is driven by the shaker located (a) on S1, (b) on S2, or (c) on S3. Images are drawn in dB using a 30 dB dynamic.

(W/m). Δ is adjusted at 10 cm for all the following results.

For each excitation point (S1, S2, and S3) which simulates an active string, the acoustic power versus frequency is computed along the y-axis and is shown in Fig. 7. These maps thus represent acoustical sources on the central line of the concert harp, where the strings are attached. It is striking that acoustical sources are found exclusively on the harp (shown by two dashed lines on the maps).

Below 750 Hz, the three maps shown in Fig. 7 are found to be similar (according to the sources location on the soundboard and their frequencies), whereas above 750 Hz they are quite different because of the potential erroneous ghost images as explained in Sec. III D. Afterwards, results are only discussed below 750 Hz, and this area is hatched in Fig. 7. In details, some discrepancies are found on these three maps due to the modal selection required by the shaker location. This selection determines not only the presence of some modes but also the acoustical sources' magnitude in the response. For example, around 600 Hz, the shaker might be connected to a particular mode's node on S1 and S2, whereas on S3 it could be attached on an anti-node, showing a high magnitude of the acoustical sources. Thus, each map represents the acoustical sources that are excited by the string which is the closest to the excitation point. That is why the strings positions on the harp and, if needed, their partials, denoted as P_i (i=2,3,...) are added to the maps (see Fig. 7).

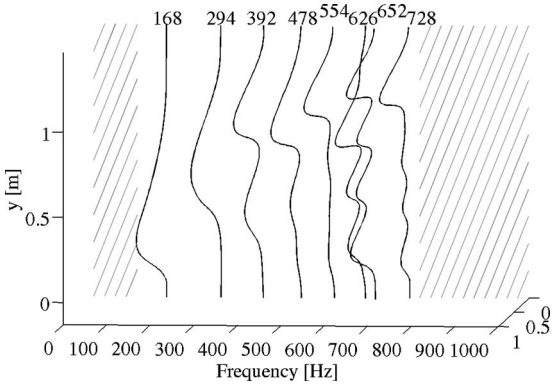

FIG. 8. Normalized acoustic power (z-axis) on the harp's central line (y-axis) for selected frequencies (x-axis).

The representations used in Fig. 7 follow Waltham and Kotlicki's paper's[1] example. In their paper, they show admittance data for different harps in order to study the string-to-string variance. They also give an interpretation of the structure of the admittance map: the soundboard is thinner in its upper part (near to the neck) than in its lower part (close to the base of the pillar). As a consequence, among the different anti-nodes of the soundboard's bending modes, the one which is in the upper part has a bigger amplitude than the others. This is illustrated in Fig. 5 of Ref. 1. This property gives the structure of the admittance map of the soundboard: when the frequency increases, the number of anti-nodes increases and the region where the admittance takes important values tends to move near to the upper part. These characteristics are also clearly visible in Fig. 8, where the acoustic power along the harp's central line (y-axis) is plotted for some frequencies. The maximum of the radiated acoustic power tends to move to the upper part of the instrument.

Thanks to these results, we can now investigate the string-to-string variance in the far field acoustic radiation of the instrument, which is, in the end, the most important. Note that our approach is interesting in the sense that we identify the equivalent acoustical sources which radiate in the far field, and, are thus, the ones that the listeners are sensitive to. In the following, the link between these acoustic maps and the string's location is studied thanks to additional measurements made in playing conditions.

B. Harp's acoustic radiation in playing condition

In this section, the harp's acoustic radiation is studied in playing conditions. For that, the harp is played in the center of a circle of radius 2.35 m composed of 32 microphones placed at 1.1 m from the floor, as shown in Fig. 9. We choose to play the strings that are the closest to the shaker's location on the soundboard. With this experimental setup, we can clearly link the acoustical sources on the soundboard, shown in Fig. 7, with the radiation of the instrument when it is played.

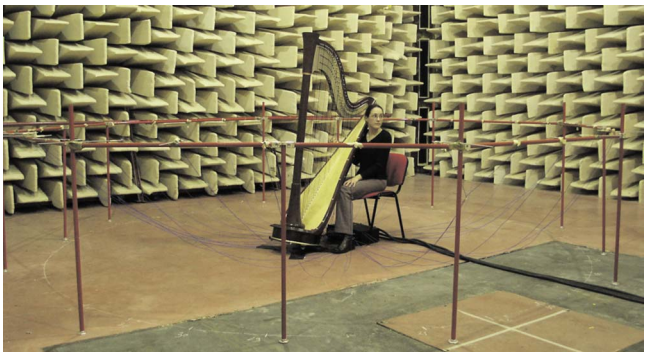

FIG. 9. (Color online) Experimental setup for the measurement of the harp's directivity when one string is played.

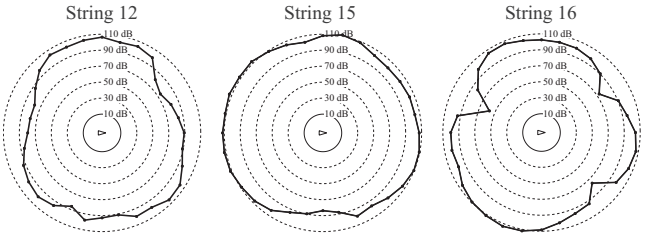

FIG. 11. Directivity patterns of the first partial computed from the first 125 ms of the temporal signal for three played strings: 12 (fundamental frequency of 813.5 Hz), 15 (606.75 Hz), and 16 (539.25 Hz) (Ref. 1 dB: 2×10^{-5} Pa).

From measured pressure around the instrument, sound levels are computed from the first 125 ms of the signal, as usually used on sound level meter[20] with a fast time constant. Patterns of radiated sound thus obtained are shown in Figs. 10 and 11 for six strings played (string 40, 31, 30, 16, 15, and 12) of fundamental frequencies from 51 to 813.5 Hz. The spatial distributions are also displayed for the fundamental frequency and for six other partials of strings 40, 31, and 30.

On the directivity patterns shown in Fig. 10, the harp is found non-directional below 255 Hz (partials 1–5 for string 40, partials 1 and 2 for string 31, and partial 1 for string 30). This result validates the two frequency ranges where the harp's directivity changes from non-directional to more complex patterns (see Sec. II B). The correspondence between the results obtained in stationary excitation and in free oscillation is not exact because of the presence of the instrumentalist behind the harp. Another interesting result shown in strings 30 and 31's patterns, is the location of the harpist's excitation point on the string. Actually, the third and the sixth partial's sound levels of strings 31 and 30 are particularly low, showing that the finger's player plucks the string at a position close to a third of the distance from the soundboard to the neck.

Apart from this remark about the plucking point, the acoustic radiation is mainly governed by the vibrational characteristics of the soundboard. At the end, these characteristics determine the acoustical sources present on the soundboard, as shown in Fig. 7. In our approach, these sources directly correspond to those that radiate in the far field. Therefore, when the string's location coincides with an acoustical source's position at the fundamental or partial's frequency of

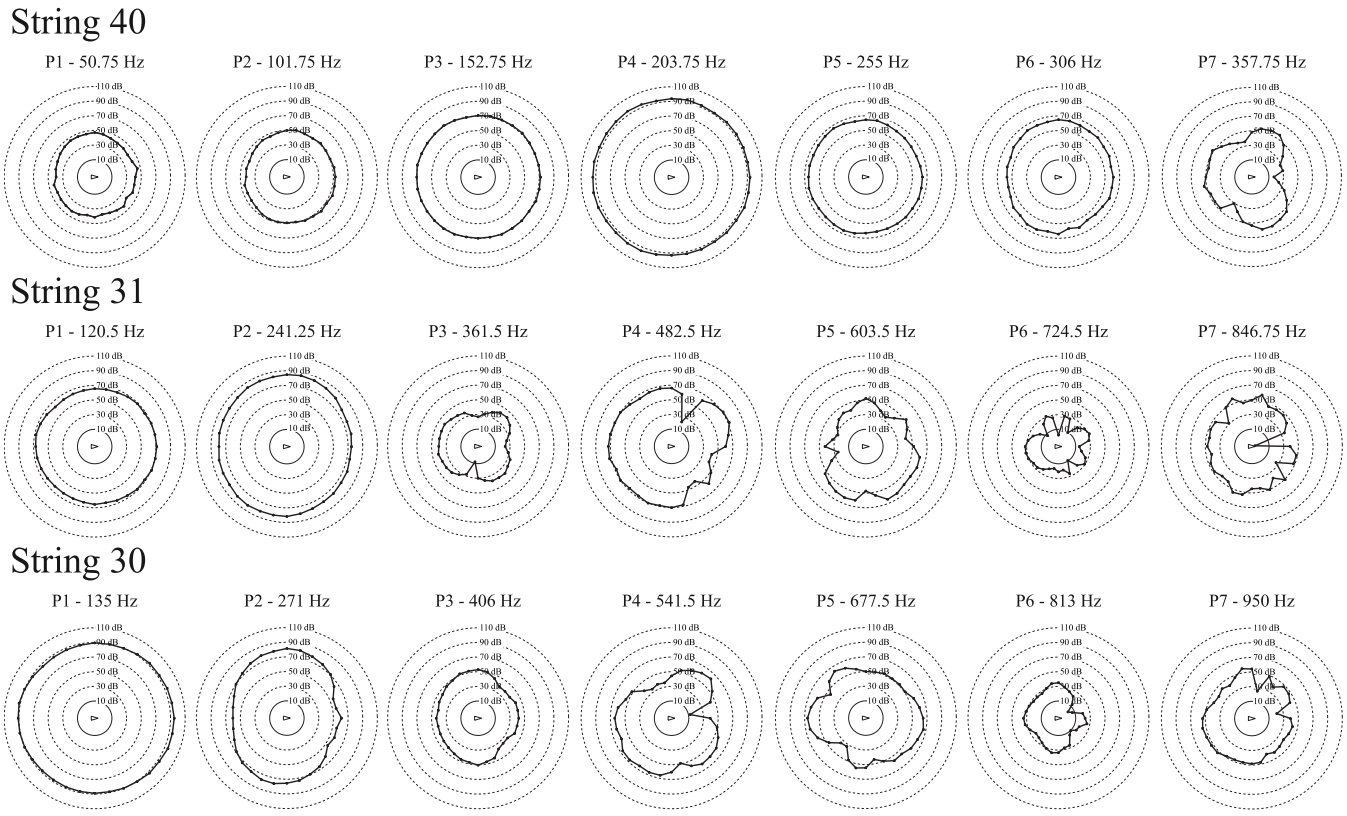

FIG. 10. Directivity patterns of seven partials P_i ($i=1,\ldots,7$) computed from the first 125 ms of the temporal signal for three played strings: 40 (fundamental frequency of 50.75 Hz), 31 (120.5 Hz), and 30 (135 Hz) (Ref 1 dB: 2×10^{-5} Pa).

the string, this note is radiated. On the contrary, if a string is far from any sources, the produced note cannot be heard. This is illustrated in directivity patterns shown in Fig. 10.

For string 40, the string's vibration is mainly radiated by partial 4 and to a lesser extent, by partial 3 due to the presence of a source at the frequency and at the location of these two partials, as shown in Fig. 7. This result demonstrates the fact that the bass strings are primarily heard through their overtones (only one overtone, in this case).

For string 31, partials 1 and 2 are mainly radiated and for string 30, it is mainly partial 1 (see Fig. 7). The acoustical sources present in the instrument determine the acoustic magnitude and directivity of each string's partial in the far field radiated sound, which can have some consequences in the spectral balance of the perceived sound. This is important in the string-to-string variance in the timbre of each string of the instrument. In their paper,[1] Waltham and Kotlicki concluded that the coincidences between strings' fundamental frequencies and the anti-nodes of the soundboard, which is correlated with excessively loud strings and, on the contrary, the coincidence between strings' fundamental frequencies and the nodes of the soundboard correlate with dead strings. We show in our study that this is more complicated, in the sense that the string's partials are also important. For strings 30 and 31, their location on the soundboard is closed but the acoustical radiation is really different for each partial. These two strings thus have different spectral balances and so string-to-string timbre variances as explained by Meyer:[8] "a variation in level of 3 dB is not very important for the loudness of a tone, but the variation in single harmonics by 3 dB has an influence on the timbre of the instrument."

In Fig. 11, the influence of the string's location on the soundboard and its frequency is clearly highlighted. Actually, the global level radiated for strings 12 and 16, located far from sources (as shown in Fig. 7(c)), is less than that of string 15 directly located on acoustical sources. Moreover, at these frequencies, a combination of several sources with different magnitudes and phases produces significant variations in the angular directivity, as shown in Fig. 11 for these three strings, which can be perceived by the listener.

Although acoustical sources are computed for a normal force applied to the soundboard, results are found to be representative of a realistic excitation made by a professional harp player. Actually, when the harpist plucks the string, the vibration along the two polarization planes turn on the acoustical sources present on the soundboard around the string's location producing a particular acoustic radiation for each note.

V. CONCLUSION

For instrumentalists, and therefore for instrument makers, the power and the sound projection of their instrument plays an important role in its quality. These two attributes are clearly linked to the instrument's radiation. In this paper, the harp's far field radiation was studied in order to give characteristics of the sound when the harp is played. We found equivalent acoustical sources on the soundboard using an appropriate acoustic imaging technique: the IFRF method. Below 375 Hz, one monopole is sufficient to describe the sound radiated by the harp. From 100 to 550 Hz, the acoustical equivalent sources of the harp go up from the bottom to the top of the sound box. Between 550 and 750 Hz, the power is mostly located at the top of the sound board. These acoustical sources correspond to the ones that radiate in the far field. When the instrument is played, coincidences between the string's fundamental or partial's frequency and these sources on the soundboard correlate with efficient radiation of the frequency or its harmonics. The acoustical sources present in the instrument thus determine the magnitude and directivity of each string's partial in the far field radiated sound, which can have some consequences in the spectral balance of the perceived sound and so in the string-to-string timbre variance of the instrument. In order to link this variance with some aspects of the instrument's quality, it would be interesting to test a large panel of harps both in playing configuration with a psychoacoustic study and in stationary regime for identifying acoustical sources on the soundboard.

ACKNOWLEDGMENTS

The authors acknowledge the instrument maker Camac Harps for lending the concert harp, the CTTM (Le Mans Centre for Technology Transfer) where the measurements where performed, the harp player C. Thomas, and the students who have taken part in the project: E. Boboeuf, G. Desoeuvre, F. Grignon, and M. Renger. Moreover, the authors would like to thanks R. Arruda and J. Gilbert for fruitful discussions.

NOMENCLATURE

ω = pulsation in rad/s
p = acoustic pressure at a microphone position
q = monopole volumetric velocity
q_i = monopole i volumetric velocity
$\tilde{p}_i$ = acoustic pressure generated by all monopoles except monopole i (but including its image by the floor) at its position
c = speed of sound
r = distance between a monopole and a microphone position
r' = distance between the image by the floor of a monopole and a microphone position
R_{ik} = distance between monopole i and monopole k
R'_{ik} = distance between monopole i and the image by the floor of monopole k
N = total number of monopoles
h = free field transfer function between a monopole and a microphone position
h' = free field transfer function between the image by the floor of a monopole and a microphone position
H = transfer function between a monopole and a microphone position including the reflection from the floor

$\mathbf{q}$ = vector of volumetric velocities q of several monopoles

$\mathbf{p}$ = vector of acoustic pressures p at several microphone positions

$\mathbf{H}$ = matrix of transfer function H between several monopoles and several microphone positions

$\mathbf{U}, \mathbf{S}, \mathbf{V}$ = matrix resulting from the singular value decomposition of $\mathbf{H}$

β = regularization parameter

$\mathbf{q}_\beta$ = regularized identified source strengths

$\mathbf{q}_0$ = identified source strengths without regularization ($\beta=0$)

η = log of the normalized energy of the solution $\mathbf{q}_\beta$

ρ = log of the normalized least-squares error

[1]C. Waltham and A. Kotlicki, "Vibrational characteristics of harp soundboards," J. Acoust. Soc. Am. **124**, 1774–1780 (2008).

[2]N. H. Fletcher and T. D. Rossing, *The Physics of Musical Instruments*, 2nd ed. (Springer, New York, 1998).

[3]A. J. Bell, "An acoustical investigation of the concert harp," Ph.D. thesis, University of St. Andrews, St. Andrews, UK, 1987.

[4]A. J. Bell and I. M. Firth, "The directivity of the concert harp," Acustica **69**, 26–30 (1989).

[5]J.-L. Le Carrou, F. Gautier, and E. Foltête, "Experimental study of A0 and T1 modes of the concert harp," J. Acoust. Soc. Am. **121**, 559–567 (2007).

[6]J.-L. Le Carrou, F. Gautier, J. Gilbert, and J. R. F. Arruda, "Low Frequency Model of the Sound Radiated by a Concert Harp," in Proceedings of the Forum Acusticum, Budapest, Hungary (2005).

[7]P. M. Morse and K. U. Ingard, *Theoretical Acoustics* (Princeton University Press, Princeton, NJ, 1986).

[8]J. Meyer, "Directivity of the bowed stringed instruments and its effect on orchestral sound in concert halls," J. Acoust. Soc. Am. **51**, 1994–2009 (1972).

[9]G. Weinreich, "Directional tone color," J. Acoust. Soc. Am. **101**, 2338–2346 (1997).

[10]J. Billingsley and R. Kinns, "The acoustic telescope," J. Sound Vib. **48**, 485–510 (1976).

[11]E. G. Williams, J. D. Maynard, and E. Skudrzyk, "Sound source reconstructions using a microphone array," J. Acoust. Soc. Am. **68**, 340–344 (1980).

[12]G. H. Koopmann, L. Song, and J. B. Fahnline, "A method for computing acoustic fields based on the principle of wave superposition," J. Acoust. Soc. Am. **86**, 2433–2438 (1989).

[13]S. M. Dumbacher and L. D. Brown, "Source imaging of irregularly shaped surfaces using inverse FRF method," in Proceedings of the ISMA 21, Leuven, Belgium (1996).

[14]C. Langrenne and A. Garcia, "Solving of the inverse problem through a Tikhonov regularization method for an acoustic source with arbitrarily shaped surfaces," in Proceedings of the Inter-Noise, Budapest, Hungary (1997).

[15]P. A. Nelson and S. H. Yoon, "Estimation of acoustic source strength by inverse methods: Part 1, Conditioning of the problem," J. Sound Vib. **233**, 639–664 (2000).

[16]P. C. Hansen, *Rank-Deficient and Discrete Ill-Posed Problems* (Society for Industrial and Applied Mathematics, Philadelphia, PA, 1998).

[17]Q. Leclere, "Acoustic imaging of complex sources with limited measurement capabilities," in Proceedings of the Euronoise, Tampere, Finland (2006).

[18]F. Gautier and N. Dauchez, "Acoustic intensity measurement of the sound field radiated by a concert harp," Appl. Acoust. **65**, 1221–1231 (2004).

[19]Q. Leclère, "Acoustic imaging using under-determined inverse approaches: Frequency limitations and optimal regularization," J. Sound Vib. **321**, 605–619 (2009).

[20]R. W. Krug, "Sound level meters," in *Encyclopedia of Acoustics*, edited by M. J. Crocker (John Wiley and Sons, Chichester, New York, 1997).